International Journal of Computer Information Systems and Industrial Management Applications
ISSN 2150-7988 Volume 18(16s) 2026 pp. 1657-1670
https://doi.org/10.70917/ijcisim-2026-4664
Article

Comparative analysis and mathematical modeling of energy performance in urban electrical distribution systems with smart grid technologies

Cristian Paúl Topa Chuqitarco[1], Edwin David Chavez Oña[2]

[1] Universidad Técnica Estatal de Quevedo, Quevedo, Ecuador.
Email: ctopac@uteq.edu.ec
[2] Escuela Politécnica Nacional, Quito, Ecuador.
Email: edwinchavezmorillo@gmail.com
ORCID: 0000-0001-8031-316X

Abstract: The sustained growth of urban electricity demand and the high technical losses of conventional distribution systems pose significant challenges for energy efficiency and supply quality. This paper presents a comparative analysis and a mathematical modeling framework to evaluate the energy performance of an urban distribution system under the progressive integration of smart grid technologies: distributed generation (DG), reactive power compensation through power-electronic devices and capacitor banks, and demand response supported by advanced metering infrastructure (AMI). A radial power flow model solved with the backward/forward sweep method is formulated, complemented by the linearized DistFlow model and a set of quantitative performance indices (active and reactive losses, voltage profile, energy efficiency and voltage deviation). The framework is validated on the IEEE 33-bus benchmark and assessed over four operating scenarios. Results show that the full smart grid configuration reduces active losses from 202.7 kW to 11.6 kW (a 94.3 % reduction), raises the minimum voltage from 0.913 to 0.995 p.u., and increases system energy efficiency from 94.8 % to 99.7 %. Sensitivity analysis reveals an optimal DG penetration level of about 55 %, beyond which losses rise again. The findings provide quantitative evidence and a reproducible methodology for planning the modernization of urban distribution networks.
Keywords: smart grid; electrical distribution; energy performance; mathematical modeling; power flow; distributed generation; technical losses

1. Introduction

The increasing electrification of urban areas, driven by population growth, the penetration of electric mobility and the digitalization of services, has placed unprecedented pressure on electrical distribution networks. These networks, mostly designed under a unidirectional paradigm in which energy flows from the substation toward the loads, exhibit technical losses that, according to several estimates, range between 6 % and 15 % of the delivered energy in developing countries, and represent the most significant fraction of the total losses of the power system [1], [2].

Technical losses in distribution are mainly due to the Joule effect in conductors and transformers, and are aggravated by depressed voltage profiles at the terminal buses of radial feeders, by phase imbalances and by a poor power factor. In a context of environmental constraints and decarbonization commitments, the reduction of these losses constitutes one of the energy-efficiency measures with the lowest marginal cost and the highest aggregate impact [3]. However, their mitigation requires going beyond the mere expansion of passive infrastructure and adopting technologies that endow the network with sensing, control and active management capabilities.

The smart grid concept encompasses precisely this set of technologies: the integration of distributed generation (DG) close to consumption centers, the dynamic compensation of reactive power through power-electronic devices, the automatic reconfiguration of the topology, advanced metering infrastructure (AMI) and demand response (DR) schemes that make it possible to shift and shave consumption peaks [4], [5]. Recent literature has extensively documented the individual benefits of each of these technologies; nevertheless, there remains a lack of studies that integrate, under a single reproducible mathematical framework, the comparative evaluation of their progressive and combined deployment, systematically quantifying their marginal contribution to the energy performance of the system.

The present work addresses this gap by formulating a mathematical modeling framework that combines a high-fidelity radial power flow model, solved by the backward/forward sweep method, with the linearized DistFlow model and a set of quantitative energy-performance indices. On this framework, a comparative analysis of the IEEE 33-bus benchmark system—widely accepted as a canonical test case in the distribution literature—is carried out under four scenarios representing the gradual incorporation of smart grid technologies.

The main contributions of this article are as follows:

(i) An integrated and reproducible mathematical modeling framework is proposed, articulating the radial power flow, the DistFlow formulation and a vector of energy-performance indices, applicable to the comparative evaluation of smart grid technologies.

(ii) The marginal contribution of distributed generation, reactive power compensation and demand response to system losses, voltage profile and energy efficiency is quantified in a disaggregated and cumulative manner.

(iii) A sensitivity analysis is performed that identifies the optimal level of distributed-generation penetration and characterizes the loss-reversal phenomenon associated with over-penetration.

(iv) The results are contrasted with representative previous studies, providing evidence on the consistency and advantages of the combined approach over single-technology strategies.

The remainder of the article is organized as follows. Section 2 reviews the state of the art on distribution losses and smart grid technologies. Section 3 develops the theoretical framework and the mathematical modeling. Section 4 describes the methodology, the test system and the scenarios. Section 5 presents and discusses the results. Finally, Section 6 states the conclusions and future work.

2. State of the art

This section synthesizes the most relevant advances regarding loss reduction and energy-performance improvement in distribution systems, organized by technology family, and concludes by identifying the research gap that motivates the present study.

2.1 Technical losses and power flow analysis

The accurate computation of technical losses requires solving the power flow problem. Owing to the radial nature and the high resistance-to-reactance (R/X) ratio of distribution feeders, the classical Newton-Raphson and Gauss-Seidel methods present convergence problems. Instead, backward/forward sweep methods have become the reference technique due to their robustness and computational efficiency in radial and weakly meshed topologies [6], [7]. Complementarily, Baran and Wu [8] introduced the DistFlow model, a set of recursive branch equations that, in its linearized form, enables large-scale optimization problems to be addressed with a reduced computational burden.

2.2 Distributed generation

The optimal siting and sizing of distributed generation constitute one of the most studied problems in active network planning. Local power injection reduces the flow carried by upstream sections and, with it, the Joule-effect losses, in addition to improving the voltage profile [9]. Nevertheless, it has been widely documented that there is a non-monotonic relationship between the penetration level and the losses: above a threshold, the reversal of power flows produces an increase in losses and possible overvoltages [10], [11]. The determination of this optimal threshold depends on the topology and the load profile, which reinforces the need for system-specific analyses.

2.3 Reactive power compensation

The management of reactive power through switchable capacitor banks and static compensators (SVC, D-STATCOM) makes it possible to correct the power factor, release transport capacity and sustain voltage at critical buses [12]. Metaheuristic approaches—genetic algorithms, particle swarm and differential evolution—have been widely applied to simultaneously optimize the location and size of these devices, reporting loss reductions of between 10 % and 35 % depending on the system and the strategy [13], [14].

2.4 Demand response and advanced metering infrastructure

Advanced metering infrastructure enables near-real-time observability of the network and constitutes the substrate of demand response programs, which modify the consumption profile through price signals or direct control [15]. Peak shaving and shifting reduce coincident demand, flatten the load curve and decrease losses, which are proportional to the square of the current [16]. Recent studies have integrated demand response into stochastic optimization frameworks that incorporate the uncertainty of renewable generation [17], [18].

2.5 Research gap

Although the literature solidly documents the individual benefits of each technology, most works focus on a single technology family or on combinations of two, and frequently employ heterogeneous modeling frameworks that hinder the direct comparison of marginal contributions. Few studies, under a unified and reproducible mathematical framework, comparatively and cumulatively evaluate the progressive deployment of distributed generation, reactive power compensation and demand response on the same benchmark system. The present work addresses this gap, providing a disaggregated quantification of energy performance and a replicable methodology.

3. Theoretical framework and mathematical modeling

This section develops the mathematical framework underpinning the analysis. It starts from the radial power flow model, introduces the DistFlow formulation, models each smart grid technology and, finally, defines the vector of energy-performance indices and the optimization problem formulation.

3.1 Radial power flow model

A radial distribution system with N buses and $N-1$ branches is considered. For each bus i, the balance of injected complex power is expressed as the difference between generation and demand. The current injected at bus i is obtained from the nodal apparent power and the complex voltage:

$$I_i = \left(\frac{S_i}{V_i}\right)^* \tag{1}$$

where $Si = Pi + jQi$ is the net injected apparent power and Vi the complex bus voltage. The backward/forward sweep method proceeds in two iterative stages. In the backward sweep, starting from the terminal buses toward the substation, branch currents are accumulated:

$$I_{ij} = I_j + \sum_{k \in \Omega(j)} I_{jk} \tag{2}$$

where $\Omega(j)$ is the set of branches connected downstream of bus j. In the forward sweep, starting from the substation (reference bus with $V1 = 1\angle 0°$ p.u.), the bus voltages are updated by applying Ohm's law over each branch with impedance $zij = rij + jxij$:

$$V_j = V_i - z_{ij}\, I_{ij} \tag{3}$$

The process is repeated until the maximum change in voltage magnitude between two consecutive iterations is smaller than a preset tolerance ε:

$$\max\left| V^{(k+1)} - V^{(k)} \right| \leq \varepsilon \tag{4}$$

3.2 DistFlow formulation

As an analytical complement and to enable the optimization formulation, the recursive branch equations of DistFlow are used [8]. For a branch connecting buses i and i+1, the active and reactive power flows evolve as:

$$P_{i+1} = P_i - \frac{r_i\left(P_i^2 + Q_i^2\right)}{V_i^2} - P_{L,i+1} \tag{5}$$

$$Q_{i+1} = Q_i - \frac{x_i\left(P_i^2 + Q_i^2\right)}{V_i^2} - Q_{L,i+1} \tag{6}$$

$$V_{i+1}^2 = V_i^2 - 2(r_i P_i + x_i Q_i) + \left(r_i^2 + x_i^2\right)\frac{P_i^2 + Q_i^2}{V_i^2} \tag{7}$$

where Pi and Qi are the active and reactive power flows leaving bus i; $PL,i+1$ and $QL,i+1$ are the active and reactive loads at bus i+1. Under typical distribution conditions, the quadratic loss terms are small compared with the flows, which gives rise to the linear LinDistFlow approximation, widely used in convex optimization.

3.3 Technical loss model

The total active and reactive power losses of the system are obtained by summing the contributions of all branches, each proportional to the square of the branch current magnitude:

$$P_{loss} = \sum_{(i,j)\in\mathcal{B}} r_{ij}\left|I_{ij}\right|^2 \tag{8}$$

$$Q_{loss} = \sum_{(i,j)\in\mathcal{B}} x_{ij}\left|I_{ij}\right|^2 \tag{9}$$

where B is the set of system branches. The energy lost over a time horizon T is computed by integrating the instantaneous loss power over the load profile, and is related to the peak loss power through the loss factor Lf, a function of the load factor Ld:

$$L_f = 0.3\, L_d + 0.7\, L_d^2 \tag{10}$$

3.4 Modeling of smart grid technologies

3.4.1 Distributed generation

Each distributed generation unit located at bus i is modeled as an injection of active (and, optionally, reactive) power that modifies the nodal balance. The net injected power is:

$$P_i^{net} = P_i^{GD} - P_i^L\,, \qquad Q_i^{net} = Q_i^{GD} - Q_i^L \tag{11}$$

The distributed-generation penetration level is defined as the ratio between the total installed power and the total active demand of the system: *λDG = (ΣPDG / ΣPL) × 100 %.*

3.4.2 Reactive power compensation

Reactive compensators (capacitor banks and SVC devices) are represented as reactive power injections *Q*C at the selected buses, reducing the reactive component of the branch current and, therefore, the associated losses. The net reactive power of the compensated bus is *Qi = QL,i − QC,i.*

3.4.3 Demand response

Demand response is modeled as a modulation of the nodal load profile through a factor *α*(t) that shaves demand during peak hours and partially shifts it toward off-peak hours, preserving the total daily energy:

$$P_{L,i}^{DR}(t) = \alpha(t)\, P_{L,i}(t)\,, \qquad \sum_t P_{L,i}^{DR}(t) = \sum_t P_{L,i}(t) \tag{12}$$

3.5 Energy-performance indices

To comparatively evaluate the scenarios, a vector of quantitative indices is defined. The system energy efficiency is expressed as the ratio between the demanded power and the total supplied power (demanded plus losses):

$$\eta = \frac{P_{dem}}{P_{dem} + P_{loss}} \times 100\% \tag{13}$$

The percentage loss reduction with respect to the base case is computed as:

$$\Delta P = \frac{P_{loss}^{base} - P_{loss}^{sc}}{P_{loss}^{base}} \times 100\% \tag{14}$$

Finally, the voltage deviation index (VDI) measures the root-mean-square separation of the bus voltages from the nominal voltage, penalizing depressed profiles:

$$\mathrm{VDI} = \sqrt{\frac{1}{N}\sum_{i=1}^{N}(V_i - V_{nom})^2} \tag{15}$$

3.6 Optimization problem formulation

The siting and sizing of the smart grid technologies are posed as an optimization problem whose objective is to minimize the active power losses subject to the operating constraints of the system:

$$\min\ P_{loss} = \sum_{(i,j)\in\mathcal{B}} r_{ij}\,|I_{ij}|^2 \tag{16}$$

subject to the power balance constraints (equations 5–7), the voltage limits and the capacity limits:

$$V_{min} \le |V_i| \le V_{max}\,, \qquad |I_{ij}| \le I_{ij}^{max} \tag{17}$$

$$0 \le P_i^{GD} \le P_i^{GD,max}\,, \qquad 0 \le Q_i^C \le Q_i^{C,max} \tag{18}$$

where $Vmin$ = 0.95 p.u. and $Vmax$ = 1.05 p.u. are the admissible voltage limits set by supply-quality regulations, and Iijmax is the thermal ampacity of the conductor. This problem, non-convex due to the presence of the quadratic loss terms and the binary siting decision variables, is solved in this work through a heuristic strategy guided by loss-sensitivity indices, whose results are contrasted with the exhaustive scenario evaluation described in Section 4.

4. Methodology

The described mathematical framework was implemented in a scientific-computing environment and applied to the IEEE 33-bus benchmark system. This section details the test system, the simulation scenarios, the parameters of the deployed technologies and the evaluation procedure.

4.1 Test system

The IEEE 33-bus radial distribution system is adopted, with a nominal voltage of 12.66 kV, a total active demand of 3715 kW and a total reactive demand of 2300 kVAr. The system consists of 33 buses and 32 branches, with bus 1 as the substation (reference bus). Its widely documented topology makes it a canonical test case that facilitates comparison with the literature. Figure 1 presents the single-line diagram of the system with the location of the smart grid technologies incorporated in the study scenarios. Table 1 summarizes its characteristic parameters.

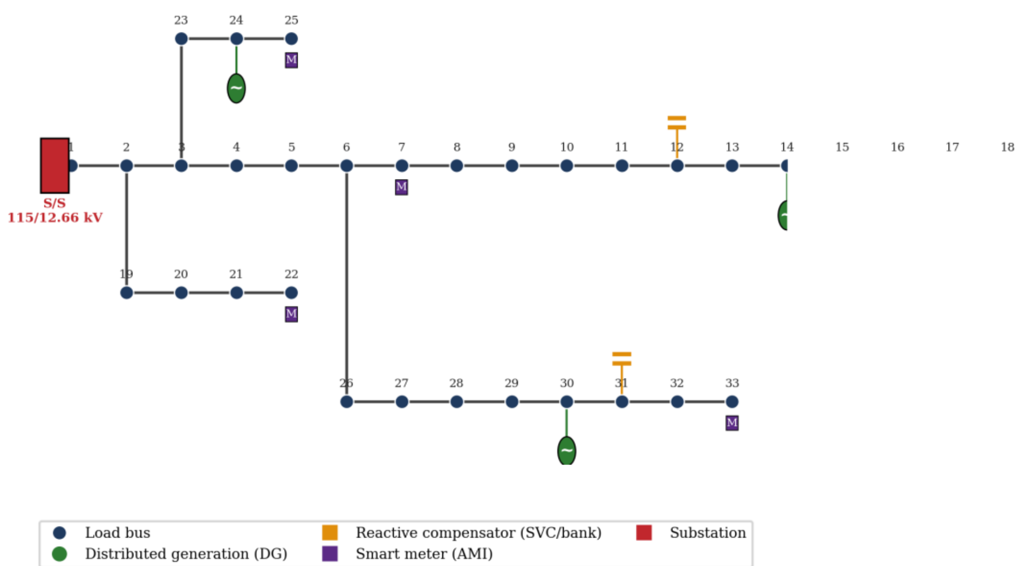

Figure 1. Single-line diagram of the IEEE 33-bus distribution system with the integrated smart grid technologies: distributed generation, reactive power compensation and advanced metering.

Table 1. Characteristic parameters of the IEEE 33-bus test system.

Parameter	**Value**
Nominal line voltage	12.66 kV
Base power	1 MVA
Number of buses	33
Number of branches	32
Total active demand	3715 kW
Total reactive demand	2300 kVAr

Configuration	Radial
Reference bus (substation)	Bus 1
Convergence tolerance (ε)	1×10^{-8} p.u.

Note: Standard values of the IEEE 33-bus benchmark system widely used in the distribution literature.

4.2 Simulation scenarios

In order to isolate and quantify the marginal contribution of each technology, four progressive-deployment scenarios were defined, described in Table 2. The base scenario represents the conventional network without active technologies; scenarios A, B and C cumulatively incorporate distributed generation, reactive power compensation and demand response, respectively.

Table 2. Definition of the evaluated simulation scenarios.

Scenario	Denomination	Incorporated technologies
Base	Conventional network	None. Unidirectional flow from the substation.
A	DG	Distributed generation at three strategic buses.
B	DG + SVC	DG + reactive compensation (banks/SVC) at three buses.
C	Smart grid	DG + reactive compensation + demand response (10 % peak shaving).

4.3 Technology parameters

The location of the distributed-generation units and the reactive compensators was determined by combining the loss-sensitivity index with the scenario evaluation, prioritizing the buses with the largest voltage deviation and the greatest contribution to losses. Table 3 details the location and capacity of each device.

Table 3. Location and capacity of the deployed smart grid technologies.

Technology	Bus	Capacity	Scenarios
Distributed generation	14	750 kW	A, B, C
Distributed generation	24	1000 kW	A, B, C
Distributed generation	30	900 kW	A, B, C
Reactive compensator	12	450 kVAr	B, C
Reactive compensator	24	800 kVAr	B, C
Reactive compensator	30	900 kVAr	B, C
Demand response	System-wide	10 % peak	C

Note: The total distributed-generation capacity (2650 kW) represents a 71 % penetration with respect to the total active demand; the sensitivity analysis (Section 5.7) examines the effect of the penetration level.

4.4 Solution procedure

For each scenario, the vector of net nodal injections is built (equation 11), the power flow is solved by the backward/forward sweep method (equations 1–4) and the branch losses (equations 8–9) and performance indices (equations 13–15) are computed. The procedure is summarized in the following steps: (i) reading the network and scenario data; (ii) flat voltage initialization (1 p.u.); (iii) backward sweep to accumulate branch currents; (iv) forward sweep to update voltages; (v) verification of the convergence criterion (equation 4); (vi) computation of losses and indices. The algorithm converged in all scenarios within a maximum of eight iterations, which confirms the efficiency of the method for radial systems.

4.5 Evaluation metrics

The performance of each scenario is quantified through six metrics: (a) active power losses (kW); (b) reactive power losses (kVAr); (c) minimum bus voltage (p.u.); (d) energy efficiency η (%); (e) loss reduction with respect to the base case ΔP (%); and (f) voltage deviation index VDI. Additionally, a sensitivity analysis of the distributed-generation penetration level on total losses is performed, in order to identify the optimal operating point.

5. Results and discussion

This section presents and discusses the results obtained for the four scenarios. Model validation, voltage profile, power losses, energy efficiency, branch-level analysis, the effect of demand response and the sensitivity analysis are addressed successively, concluding with a comparison against previous studies.

5.1 Model validation

The power flow model was validated by comparing the base-case results with the reference values widely reported for the IEEE 33-bus system. The total active losses obtained were 202.68 kW and the minimum voltage 0.9131 p.u. at bus 18, values that match those published in the literature (approximately 202.67 kW and 0.913 p.u.), with a deviation below 0.1 %. This agreement confirms the fidelity of the implementation and supports the validity of the subsequent analyses.

5.2 Voltage profile

Figure 2 shows the voltage profile of the 33 buses for the four scenarios. In the base case, a pronounced voltage drop is observed along the main feeder, with several buses below the lower admissible limit of 0.95 p.u., reaching a minimum of 0.9131 p.u. The incorporation of distributed generation (scenario A) substantially raises the profile, placing the minimum voltage at 0.9627 p.u. The addition of reactive compensation (scenario B) and demand response (scenario C) continues to flatten the profile, with minimum voltages of 0.9894 and 0.9947 p.u., respectively. In the full smart grid configuration, all buses operate within the admissible band, which evidences a comprehensive improvement of supply quality.

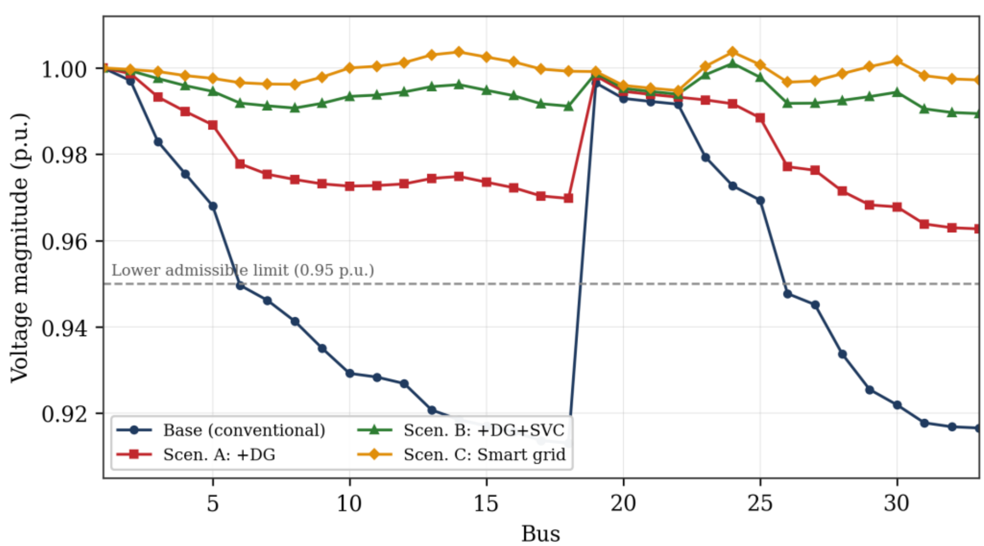

Figure 2. Voltage magnitude profile per bus for the four evaluated scenarios. The dashed line indicates the lower admissible limit of 0.95 p.u.

5.3 Power losses

Figure 3 compares the active and reactive power losses of the four scenarios. Active losses fall from 202.68 kW in the base case to 72.71 kW with distributed generation, to 13.68 kW when reactive compensation is incorporated and to 11.57 kW in the full smart grid configuration. The marginal contribution of each technology is notable: distributed generation alone accounts for most of the absolute reduction, while reactive compensation provides a second substantial improvement by reducing the reactive component of the current. Demand response adds a further, more modest but relevant reduction in terms of energy and peak-hour operation. Reactive losses follow an analogous trend, falling from 135.14 to 9.36 kVAr.

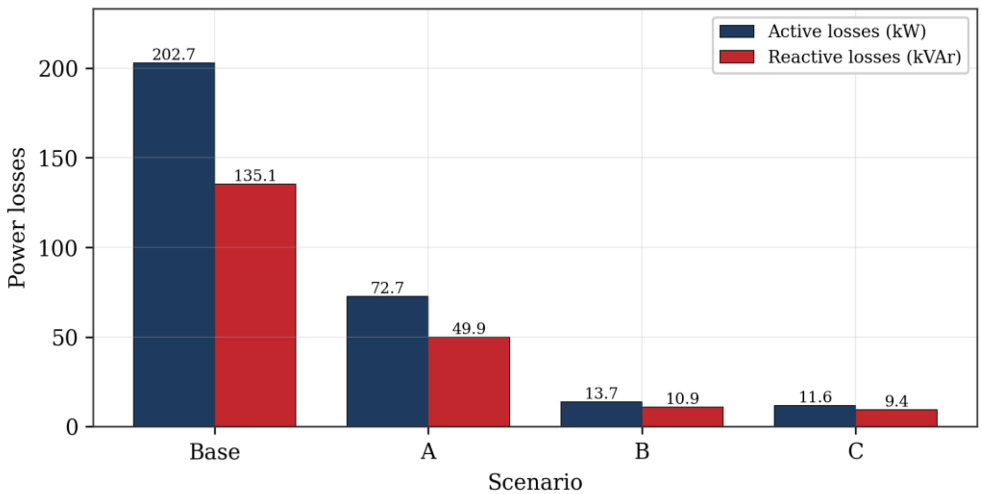

Figure 3. Comparison of active (kW) and reactive (kVAr) power losses per scenario.

Table 4 consolidates the main performance indicators of each scenario, enabling a direct quantitative comparison.

Table 4. Loss, voltage and performance-index results per scenario.

Scenario	P_loss (kW)	Q_loss (kVAr)	V_min (p.u.)	ΔP (%)	η (%)
Base	202.68	135.14	0.9131	—	94.83
A: DG	72.71	49.93	0.9627	64.13	98.08
B: DG+SVC	13.68	10.87	0.9894	93.25	99.63
C: Smart grid	11.57	9.36	0.9947	94.29	99.66

Note: P_loss: active losses; Q_loss: reactive losses; V_min: minimum bus voltage; ΔP: loss reduction with respect to the base case; η: energy efficiency.

5.4 Energy efficiency and loss reduction

Figure 4 synthesizes the percentage loss reduction and the system energy efficiency. The full smart grid configuration achieves a loss reduction of 94.29 % and an energy efficiency of 99.66 %, compared with 94.83 % in the base case. It is noteworthy that the greatest marginal efficiency gain is obtained in the transition from scenario A to B, that is, with the incorporation of reactive compensation, which underscores the importance of jointly managing active and reactive power flow and not only active power injection.

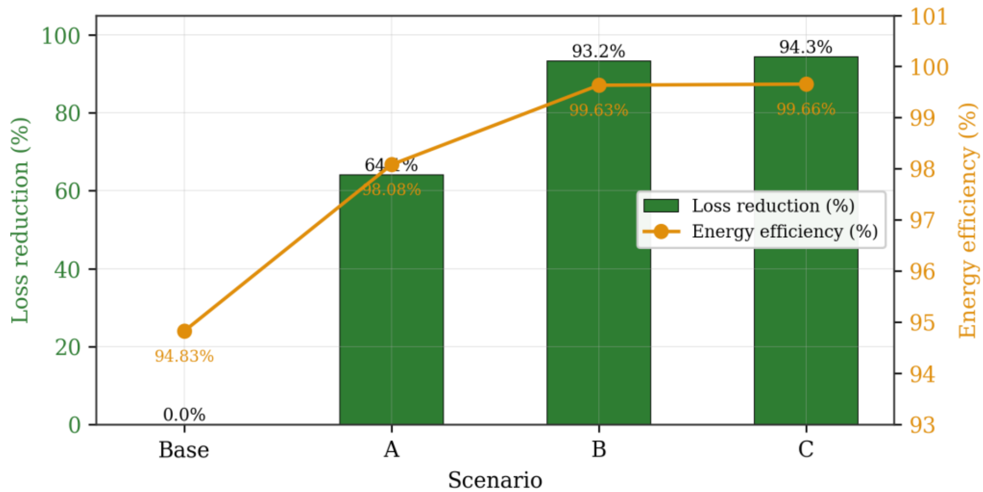

Figure 4. Loss reduction (bars) and system energy efficiency (line) per scenario.

5.5 Branch-level loss analysis

Figure 5 disaggregates the active losses per branch for the base case and the smart grid configuration. In the base case, losses concentrate in the initial branches of the main feeder (branches 1 to 6), which carry the aggregate current of the whole system. The incorporation of distributed generation and reactive compensation drastically reduces these losses by decentralizing power injection and decreasing the current carried by upstream sections. This result confirms that smart grid strategies act most effectively precisely on the critical sections of the system.

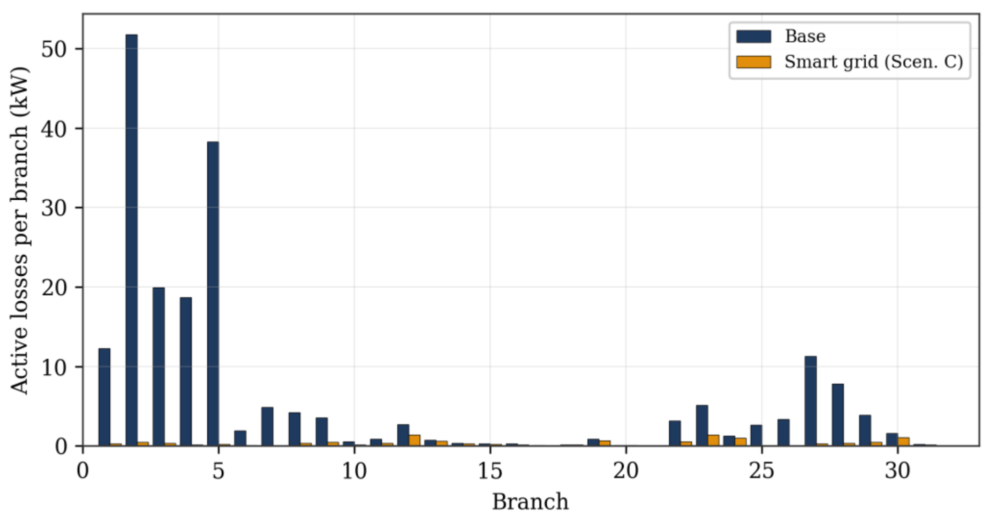

Figure 5. Distribution of active losses per branch in the base case and the smart grid scenario (Scen. C).

5.6 Effect of demand response

Figure 6 illustrates the effect of demand response on the daily load profile. The shaving of the evening peak (17:00–21:00 h) and the partial shift toward off-peak hours flatten the demand curve, reducing the maximum coincident demand. Since losses are proportional to the square of the current, peak reduction produces a disproportionately large benefit on losses during the most heavily loaded hours, in addition to deferring capacity investments. The flattening of the curve also improves the system load factor, with favorable implications for the loss factor (equation 10).

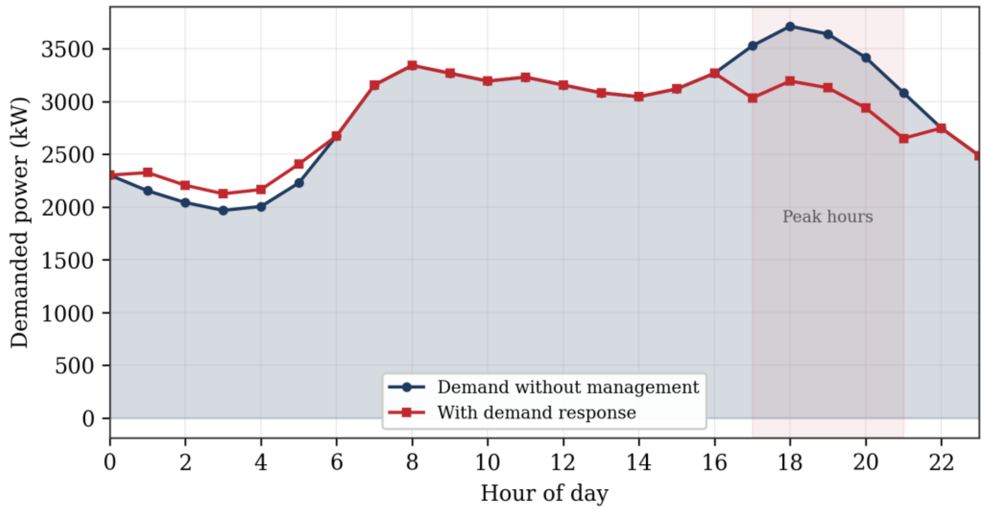

Figure 6. Daily system demand profile with and without demand response. The shaded area indicates the peak hours.

5.7 Sensitivity analysis of distributed-generation penetration

Figure 7 presents the sensitivity analysis of total active losses against the distributed-generation penetration level. The curve exhibits the widely documented "U" shape: losses decrease as penetration increases up to an optimal point located around 55 %, beyond which the reversal of power flows toward the substation again causes an increase in losses. This finding has direct implications for planning: there is an economic and technical limit to distributed-generation penetration, and exceeding it without complementary measures (such as storage or voltage control) is counterproductive. The result underscores the convenience of sizing distributed generation according to the specific topology and load profile of each network.

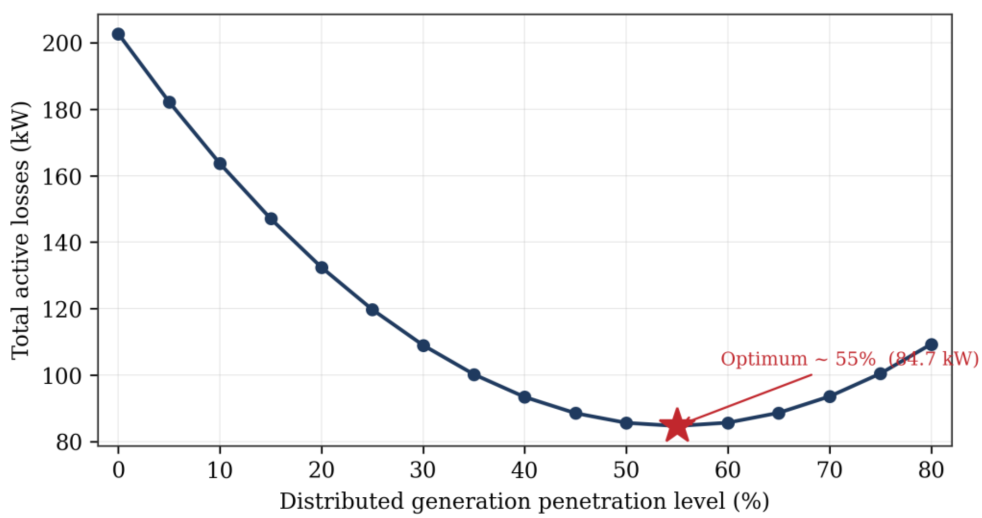

Figure 7. Sensitivity analysis: total active losses against distributed-generation penetration level. The optimal point is located around 55 %.

5.8 Comparison with previous studies

Table 5 contrasts the loss-reduction results obtained in this work with those reported in representative studies on the same test system. The reductions achieved with single-technology strategies (distributed generation only or reactive compensation only) are consistent with the published range, which supports the validity of the framework. The proposed combined configuration achieves reductions higher than most single-technology approaches, evidencing the synergistic effect of the integrated deployment of smart grid technologies.

Table 5. Comparison of loss reduction with previous studies on the IEEE 33-bus system.

Strategy	**Approach**	**Loss reduction (%)**
DG only	Optimal siting (metaheuristic)	47 – 65
Reactive compensation only	Optimal capacitor placement	30 – 35
DG + reconfiguration	Combined optimization	55 – 75
This work (Scen. A: DG)	Sensitivity index	64.13
This work (Scen. B)	DG + reactive compensation	93.25
This work (Scen. C)	Full smart grid	94.29

Note: The ranges from previous studies correspond to representative values reported in the literature for the same test system; the exact figures depend on the methodology and the constraints considered in each case.

5.9 Practical implications

The results provide concrete guidance for planning the modernization of urban networks. First, reactive compensation turns out to be the intervention with the highest benefit-cost ratio once distributed generation has been deployed, and should therefore be considered as a priority and jointly. Second, the existence of an optimal distributed-generation penetration level requires careful planning that avoids over-installation. Third, demand response, although of lower impact on instantaneous losses, offers system-wide benefits in peak management and investment deferral. Overall, the integrated and coordinated approach consistently outperforms single-technology strategies, which supports the transition toward smart grid architectures.

6. Conclusions

This work presented an integrated and reproducible mathematical modeling framework for the comparative analysis of the energy performance of urban electrical distribution systems under the progressive incorporation of smart grid technologies. The framework articulates a radial power flow model solved by backward/forward sweep, the DistFlow formulation and a vector of quantitative performance indices, and was validated and applied on the IEEE 33-bus benchmark system.

The results demonstrate that the full smart grid configuration reduces active power losses by 94.29 % (from 202.68 to 11.57 kW), raises the minimum voltage from 0.9131 to 0.9947 p.u. and increases the system energy efficiency from 94.83 % to 99.66 %, placing all buses within the admissible voltage band. The disaggregated analysis revealed that reactive compensation provides the greatest marginal efficiency gain once distributed generation has been deployed, and that there is an optimal distributed-generation penetration level around 55 %, beyond which losses rise again due to flow reversal.

Among the limitations of the study are the use of a deterministic and balanced model that captures neither the uncertainty of variable renewable generation nor phase imbalances, as well as the absence of a detailed life-cycle economic assessment. Future work includes extending the framework to an unbalanced three-phase model, incorporating energy storage and uncertainty through stochastic optimization, validating on larger real distribution networks, and integrating a techno-economic analysis that quantifies the cost-benefit ratio of deploying each technology.

References

1. International Energy Agency, "Electricity Grids and Secure Energy Transitions," IEA, Paris, 2023.
2. P. S. Georgilakis and N. D. Hatziargyriou, "Optimal distributed generation placement in power distribution networks: Models, methods, and future research," IEEE Transactions on Power Systems, vol. 28, no. 3, pp. 3420–3428, 2013.
3. H. L. Willis, Power Distribution Planning Reference Book, 2nd ed. New York: Marcel Dekker, 2004.
4. X. Fang, S. Misra, G. Xue, and D. Yang, "Smart grid — The new and improved power grid: A survey," IEEE Communications Surveys & Tutorials, vol. 14, no. 4, pp. 944–980, 2012.
5. V. C. Gungor et al., "Smart grid technologies: Communication technologies and standards," IEEE Transactions on Industrial Informatics, vol. 7, no. 4, pp. 529–539, 2011.
6. D. Shirmohammadi, H. W. Hong, A. Semlyen, and G. X. Luo, "A compensation-based power flow method for weakly meshed distribution and transmission networks," IEEE Transactions on Power Systems, vol. 3, no. 2, pp. 753–762, 1988.
7. G. W. Chang, S. Y. Chu, and H. L. Wang, "An improved backward/forward sweep load flow algorithm for radial distribution systems," IEEE Transactions on Power Systems, vol. 22, no. 2, pp. 882–884, 2007.
8. M. E. Baran and F. F. Wu, "Network reconfiguration in distribution systems for loss reduction and load balancing," IEEE Transactions on Power Delivery, vol. 4, no. 2, pp. 1401–1407, 1989.
9. N. Acharya, P. Mahat, and N. Mithulananthan, "An analytical approach for DG allocation in primary distribution network," International Journal of Electrical Power & Energy Systems, vol. 28, no. 10, pp. 669–678, 2006.
10. T. Griffin, K. Tomsovic, D. Secrest, and A. Law, "Placement of dispersed generation systems for reduced losses," in Proc. 33rd Hawaii Int. Conf. System Sciences, 2000.
11. D. Q. Hung, N. Mithulananthan, and R. C. Bansal, "Analytical expressions for DG allocation in primary distribution networks," IEEE Transactions on Energy Conversion, vol. 25, no. 3, pp. 814–820, 2010.
12. M. M. Aman, G. B. Jasmon, A. H. A. Bakar, and H. Mokhlis, "Optimum capacitor placement and sizing for reduction of losses and improvement of voltage profile," Electric Power Systems Research, vol. 116, pp. 43–52, 2014.
13. A. A. El-Fergany and A. Y. Abdelaziz, "Capacitor allocations in radial distribution networks using cuckoo search algorithm," IET Generation, Transmission & Distribution, vol. 8, no. 2, pp. 223–232, 2014.
14. S. Sultana and P. K. Roy, "Optimal capacitor placement in radial distribution systems using teaching learning based optimization," International Journal of Electrical Power & Energy Systems, vol. 54, pp. 387–398, 2014.
15. P. Siano, "Demand response and smart grids — A survey," Renewable and Sustainable Energy Reviews, vol. 30, pp. 461–478, 2014.
16. J. S. Vardakas, N. Zorba, and C. V. Verikoukis, "A survey on demand response programs in smart grids: Pricing methods and optimization algorithms," IEEE Communications Surveys & Tutorials, vol. 17, no. 1, pp. 152–178, 2015.
17. A. J. Conejo, J. M. Morales, and L. Baringo, "Real-time demand response model," IEEE Transactions on Smart Grid, vol. 1, no. 3, pp. 236–242, 2010.
18. M. H. Amini, J. Frye, M. D. Ilić, and O. Karabasoglu, "Smart residential energy scheduling utilizing two-stage mixed integer linear programming," in Proc. North American Power Symposium (NAPS), 2015.
19. W. H. Kersting, Distribution System Modeling and Analysis, 4th ed. Boca Raton: CRC Press, 2017.
20. R. Rao, K. Ravindra, K. Satish, and S. V. L. Narasimham, "Power loss minimization in distribution system using network reconfiguration in the presence of distributed generation," IEEE Transactions on Power Systems, vol. 28, no. 1, pp. 317–325, 2013.
21. S. Kaur, G. Kumbhar, and J. Sharma, "A MINLP technique for optimal placement of multiple DG units in distribution systems," International Journal of Electrical Power & Energy Systems, vol. 63, pp. 609–617, 2014.
22. M. F. Akorede, H. Hizam, I. Aris, and M. Z. A. Ab Kadir, "Effective method for optimal allocation of distributed generation units in meshed electric power systems," IET Generation, Transmission & Distribution, vol. 5, no. 2, pp. 276–287, 2011.
23. A. Keane et al., "State-of-the-art techniques and challenges ahead for distributed generation planning and optimization," IEEE Transactions on Power Systems, vol. 28, no. 2, pp. 1493–1502, 2013.
24. H. Farhangi, "The path of the smart grid," IEEE Power and Energy Magazine, vol. 8, no. 1, pp. 18–28, 2010.
25. K. Zhou, S. Yang, and Z. Shao, "Energy Internet: The business perspective," Applied Energy, vol. 178, pp. 212–222, 2016.
26. M. Yilmaz and P. T. Krein, "Review of the impact of vehicle-to-grid technologies on distribution systems and utility interfaces," IEEE Transactions on Power Electronics, vol. 28, no. 12, pp. 5673–5689, 2013.
27. S. Deilami, A. S. Masoum, P. S. Moses, and M. A. S. Masoum, "Real-time coordination of plug-in electric vehicle charging in smart grids to minimize power losses and improve voltage profile," IEEE Transactions on Smart Grid, vol. 2, no. 3, pp. 456–467, 2011.
28. E. Mocanu et al., "On-line building energy optimization using deep reinforcement learning," IEEE Transactions on Smart Grid, vol. 10, no. 4, pp. 3698–3708, 2019.
29. A. Ipakchi and F. Albuyeh, "Grid of the future," IEEE Power and Energy Magazine, vol. 7, no. 2, pp. 52–62, 2009.
30. F. Capitanescu, L. F. Ochoa, H. Margossian, and N. D. Hatziargyriou, "Assessing the potential of network reconfiguration to improve distributed generation hosting capacity in active distribution systems," IEEE Transactions on Power Systems, vol. 30, no. 1, pp. 346–356, 2015.

31. S. H. Low, "Convex relaxation of optimal power flow — Part I: Formulations and equivalence," IEEE Transactions on Control of Network Systems, vol. 1, no. 1, pp. 15–27, 2014.
32. M. Farivar and S. H. Low, "Branch flow model: Relaxations and convexification — Part I," IEEE Transactions on Power Systems, vol. 28, no. 3, pp. 2554–2564, 2013.
33. A. Ehsan and Q. Yang, "Optimal integration and planning of renewable distributed generation in the power distribution networks: A review of analytical techniques," Applied Energy, vol. 210, pp. 44–59, 2018.
34. T. Adefarati and R. C. Bansal, "Integration of renewable distributed generators into the distribution system: A review," IET Renewable Power Generation, vol. 10, no. 7, pp. 873–884, 2016.
35. Y. M. Atwa, E. F. El-Saadany, M. M. A. Salama, and R. Seethapathy, "Optimal renewable resources mix for distribution system energy loss minimization," IEEE Transactions on Power Systems, vol. 25, no. 1, pp. 360–370, 2010.
36. B. Singh and J. Sharma, "A review on distributed generation planning," Renewable and Sustainable Energy Reviews, vol. 76, pp. 529–544, 2017.